

# Tactical Weather Radar Experiment for a Shipborne Radar

H. Owen, H. Urkowitz, N. Bucci, J. Melody, and R. McLean  
Lockheed Martin Corporation, Government Electronic Systems,  
Moorestown, NJ

## Abstract:

Meteorological conditions **affect** almost every aspect of naval warfighting operations. Precipitation and winds affect the operational tempo of combat **forces at sea, during amphibious** operations, and during aviation operations. Precipitation generates a clutter environment that degrades electromagnetic and **electro-optical** sensor performance. Specific propagation paths, such as surface ducts, **can develop which greatly affect an** electromagnetic sensor's performance. **Wind fields affect ballistic** weapon trajectories and the dispersion of chemical and biological agents which **are** becoming more common as warheads. If measurements can be accurately made of environmental conditions, the warfighter can be better prepared to adjust operational schedules, sensor employment, and weapon deployment to complete a specific mission.

Using innovative signal processing techniques, Lockheed Martin Corporation, Government Electronic Systems, is currently exploring the use of a tactical multi-function shipborne radar, the AN/SPY-1 B/D, for the measurement of meteorological conditions. The SPY-1 radar's normal tactical waveforms, if processed correctly, can provide maps of reflectivity, scatterer mean radial velocity, and spectrum width (indicative of turbulence and wind shear) throughout a search volume. This can be done without interruption to the radar's tactical scan. These measurements are often referred to as the three spectral moments in radar metrology. Application of advanced signal processing techniques allow for the SPY-1 to make these measurements using coded tactical waveforms and a very small number of pulses (where traditionally uncoded waveforms and long pulse doppler dwells have been required for weather observations).

## Overview of Conventional Radar Meteorology Techniques:

The National Weather Service's newest doppler weather radar, NEXRAD, measures precipitation intensity and characteristics of wind fields of a storm. These radars have been deployed throughout the U. S., and they provide the up-to-the-minute mosaics of weather conditions now available throughout the country.

Measurements are generally made of three basic spectral moments: reflectivity (a measure of scatterer density), mean radial velocity, and spectrum width (an indicator of turbulence and shear). NEXRAD takes measurements of these characteristics using the pulse pair processing technique on data

taken from long sequences of uncoded pulses. In this technique, measurements of received signal power and characteristics of the first lag of the weather signal's autocorrelation function are used to generate estimates of the three spectral moments. It should be noted that estimates of these three moments can be made through pulse pair processing without actually generating a spectrum of the weather signal. The relationship between pairs of pulses is enough to provide information on signal intensity, mean radial velocity, and the width of the weather signal spectrum. Use of long, uncoded, multiple pulse dwells allows for the radar to take a large number of samples of a phenomenon to make accurate measurements, and it allows for clutter filtering techniques to be applied at the lowest elevation to remove the effects of ground clutter from the signal spectrum.

At this point, it is appropriate to provide a brief overview of the definitions for the three spectral moments. This discussion is largely taken from reference [1].

Estimation of the level of reflectivity in a storm is relatively straight forward. A number of samples, on the order of 100, are typically taken of the received signal power over a region of interest. These samples are averaged, and a conversion is made from received signal intensity to reflectivity, based on radar beam width, sample range, transmission power, and system losses. The reflectivity factor (a meteorological measurement) is calculated from the general radar value of reflectivity. The term "reflectivity factor" is defined as

$$Z = \frac{\eta a'}{\pi^5 |K|^2}$$

where

$\eta$  = backscattering cross section per unit volume,  
 $\lambda$  = transmitted wavelength, and  
 $|K|^2$  = a constant based on the backscatterers' index of refraction (approximately 0.93 for water phase precipitation).

The reflectivity factor is generally described on a logarithmic scale (units of dBZ), calculated as  $10 \log Z$ , where  $Z$  is in units of  $\text{mm}^6/\text{m}^3$ . Typical values range from 10 dBZ (drizzle) through 40 dBZ (rain)

to 70 dBZ (rain and hail). Nonprecipitating clouds have values ranging from -15 dBZ to -30 dBZ.

Estimation of mean radial velocity is made using an estimate of the first lag of the weather signal's autocorrelation function. Again, a number of samples (on the order of 100) are typically used to make this measurement. The estimate of the autocorrelation function is given as

$$R(T_s) = \frac{1}{M} \sum_{m=0}^{M-1} V^*(m) V(m+1).$$

where  $V(m)$  represents the complex basedband voltage samples taken at a single range position at a sample rate equal to the radar's pulse repetition interval (PRI). In the most straightforward approach, one sample is taken each pulse, so that the number of pulses becomes  $M$ . The estimate of mean radial velocity becomes

$$\mathbf{v}_r = \left( \frac{\lambda}{4\pi T_s} \right) \arg R(T_s)$$

where

$T_s$  = the pulse repetition interval (PRI).

This estimator of mean radial velocity is not biased by white noise. Even when the spectrum is not symmetric, the mean radial velocity is accurate as long as the weather signal is contained in a small band relative to the Nyquist interval which results from the sample rate. More detail of the pulse pair mean velocity estimator is provided in reference [1].

The spectrum width estimator is a function of the magnitude of the first lag of the autocorrelation function. If this value is relatively large, the signal can be considered to be more coherent (and have less spread). If it is relatively small, the signal is less coherent (and has more spread). One spectrum width estimator is given as

$$\sigma_v = \left( \frac{\lambda}{2\sqrt{2}\pi T_s} \right) \left[ \left| \ln \frac{S}{|R_1|} \right| \right]^{1/2} \operatorname{sgn} \left[ \ln \left( \frac{S}{|R_1|} \right) \right]$$

where

$R_1$  = the autocorrelation estimate evaluated for  $T_s$  equal to the waveform PRI

$S$  = the estimate of signal power (total received power minus noise power).

The accuracy of the estimates made using the pulse pair technique depends on several factors,

including signal to noise ratio (SNR), spectrum width of the signal being measured, and numbers of independent samples used in the estimation of signal power and the first lag of the autocorrelation function. Many tradeoffs can be made to optimize the spectral moment estimation accuracy.

If SNR and signal spectrum width are held constant, however, the number of independent samples becomes the main issue for spectral moment accuracy. In general, a larger number of independent samples of a signal results in improved spectral moment accuracy.

There are a number of ways to increase the number of independent samples taken of a weather event. Larger numbers of pulses can be transmitted (the most straightforward approach). Multiple transmission and receive channels can be employed to take more than one sample simultaneously. If a radar scans a region fast enough, scan to scan averaging of the spectral moments themselves can be used to reduce the estimate variance. And finally, range averaging of the samples taken can help reduce the variance of the spectral moments.

This last technique has been investigated previously, as outlined in reference [2]. Range averaging is an attractive option for collecting an increased number of samples, however it requires that smaller range resolutions be achieved for individual measurements so that range reporting intervals are not increased when these individual samples are averaged over range. Coded waveforms have traditionally been used in tactical radars to improve range resolution, but coded waveforms have not been used in operational weather radars due to the degradation of the weather measurements from range sidelobes. The range sidelobes which result from coded waveforms have the effect of "smearing" the weather picture, masking weak features or sharp reflectivity and velocity changes in the face of stronger signals which are flooded through range sidelobes.

Short, uncoded pulses could be used to achieve the better range resolution required for range averaging, but the reduction in pulse width in this approach would reduce signal to noise ratio. This would result in larger errors in the spectral moment measurements.

### Tactical Weather Radar Operation:

Many tactical radar systems share a set of common characteristics: operation at or near S-band, use of coded waveforms, use of small numbers of pulses (such as MTI waveforms) in search modes,

and good system sensitivity. These basic radar characteristics, with the proper signal processing, can produce accurate spectral moments estimates without the use of dedicated waveforms.

With pulse pair processing, it is not necessary to have 100 pulses in a dwell to make weather measurements. In the Tactical Weather Radar (TWR) concept, small numbers of pulses (typical of MTI dwells) can be used to make these measurements. Consider the case of a tactical system with the following parameters. (Note: these parameters are not necessarily reflective of the SPY-1 radar but are used here as an example and include characteristics of a number of tactical systems.)

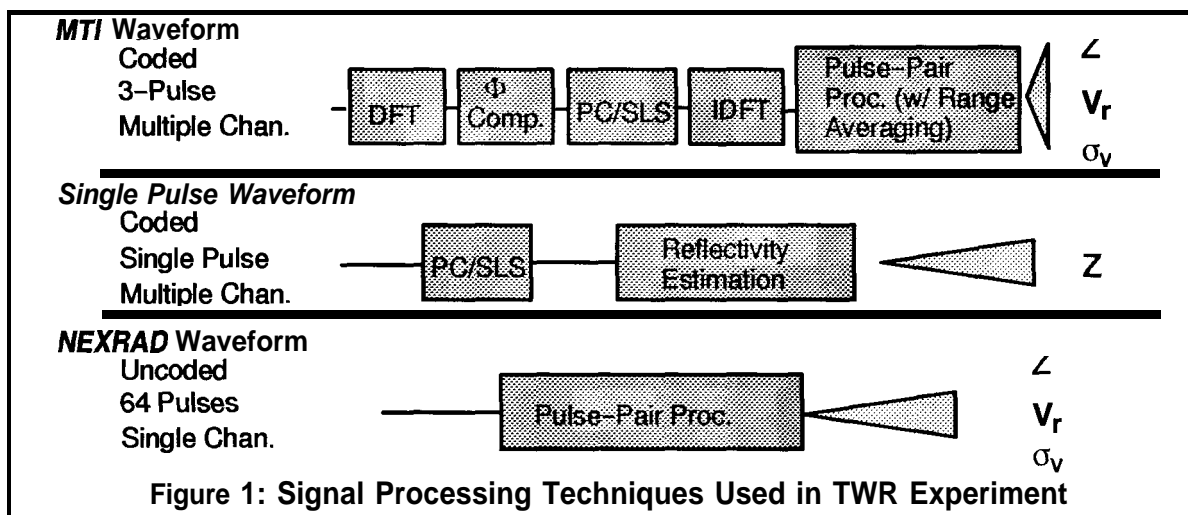
Pulse Type:	MTI
Number of Pulses:	3
# Simult. Trans/Rec Channels:	3
Range Resolution:	50 m
Reporting Range Required:	500m
Waveform Coding:	Yes

Using traditional radar processing with only pulse to pulse averaging, there would be 3 pulses and 2 pulse pair groups to make spectral moment estimates. However, this fictional tactical radar has three channels from which to collect data and 500 meters over which to average results prior to reporting the spectral moment data. Therefore, the total number of samples becomes 90 ( $3 \times 3 \times 10$ ), and the total number of pulse pairs becomes 60 ( $2$

$\times 3 \times 10$ ). Although 3 pulse samples and 2 lag samples are not adequate for estimation of the three spectral moments, 90 pulse samples and 60 lag samples are generally adequate.

The use of a coded waveform, however, poses another problem. Coded waveforms result in range sidelobes that smear weather measurements in range. Range sidelobe suppression techniques can be used to reduce the effect of range sidelobes. However, these techniques (such as sidelobe suppression filters and inverse filters) degrade quickly in the presence of doppler shifts in the received signal. Therefore, doppler tolerant techniques must be applied.

Lockheed Martin developed a doppler tolerant range sidelobe suppression technique that has been successfully demonstrated in research radars for Federal Aviation Administration (FAA) applications (see references [3], [4], [5], and [6]). A signal processor testbed has been developed as part of these investigations, and this testbed is being used to process SPY-1 data in this experiment. In the FAA case, a coded pulse doppler waveform was used to make spectral moment measurements. In this experiment, the technique is adapted for MTI waveform processing, and single pulse coded waveform processing. Consider figure 1 which illustrates the TWR signal processor testbed.



This figure outlines three of the processing approaches used in the experiment. First, a processing approach for a 3 pulse MTI system is presented. In this case, each of the simultaneous channels of the radar system is processed separately, and the results are averaged once the auto-

correlation function estimate is made. A Discrete Fourier Transform (DFT) is performed across the three samples taken at each range interval. Phase compensation is applied so that the combined pulse compression (PC) / sidelobe suppression (SLS) filter is matched to each of the three outputs

of the DFT. After PC/SLS filtering, an Inverse DFT is taken to produce the 3 pulse sequence that is used in pulse-pair processing. The results of the pulse pair processing (estimates of total signal power and the first lag of the signal's autocorrelation function) are then averaged over multiple pulses, multiple channels, and over range to produce a result which accurately reflects the weather spectrum characteristics.

The second approach is appropriate for a single pulse waveform. In a single pulse waveform, no doppler phase compensation is possible since only one pulse is transmitted. However, measurements can still be made of reflectivity. Since most tactical systems use something like MTI in regions where clutter (such as precipitation) is expected, it is probable that a multiple pulse waveform will be transmitted in regions of precipitation.

The last signal processing path represents that of the NEXRAD waveform. No pulse compression is used since the waveforms are uncoded. Almost all averaging is done over pulses. Therefore, the processing approach is simpler but requires a large number of pulses to be transmitted in each beam position to make the desired measurements (on the order of 60 or 100).

### Outline of Experiment:

The primary goal of this experiment is to determine what weather information can be gained through processing of normal, tactical search waveform data through a separate signal processor. A second goal of the experiment is to determine what dedicated dwells would be required to provide for measurements of additional phenomena not covered by typical search dwells. It is expected that dedicated weather dwells are appropriate when very low reflectivity phenomena are being observed, and when surface clutter filtering is desired to remove the effects of surface clutter from the weather spectral moment estimates.

The experiment consists of an equipment preparation period followed by three data collection phases. The equipment installation period is required to install a data tap so that raw radar data can be extracted from the signal processor and stored for post-mission processing and analysis. The first data collection phase is the Baseline data set and is required to test out the data tap, general data quality, and the software patches required to control the radar in a manner that will allow for the collection of appropriate experimental weather data. Lessons learned in this portion of the experi-

ment were applied to subsequent data collection sets to improve data collection and data processing techniques. The second data collection phase is the Proof of Concept data set, and it primarily involves the collection of precipitation data to compare the results of the SPY-1 radar with those of a nearby NEXRAD doppler weather radar taken simultaneously. It is during this phase of the experiment that SPY-1's ability to collect precipitation weather data is assessed. The last data collection phase is the Clear Air Observations data set in which specialized, dedicated waveforms will be used to investigate SPY-1's ability to detect low observable weather phenomena such as clear air turbulence and cloud layers. This paper primarily deals with data collected during the Proof of Concept data set.

Two basic types of comparisons are used in the Proof of Concept data set to determine the accuracy of SPY-1 weather measurements using tactical waveforms. First, reflectivity maps taken from a SPY-1 radar, located at the Navy's Combat System Engineering Development (CSED) Site in Moorestown, NJ, are compared with those taken from a nearby NEXRAD. The NEXRAD is located approximately 44 kilometers to the East of the SPY-1 radar. Coverage of the two radars overlaps over much of New Jersey. Data collection events were focused on central and northern New Jersey, extending past New York City to the North in some cases. Reflectivity measurements do not depend upon radar aspect relative to the phenomenon measured (assuming neither radar is attempting to make measurements beyond the radar horizon). Therefore, comparison of results from two radars is appropriate for this investigation.

When comparing radial velocity, however, radar aspect angle is important. Two radars viewing a single storm cell will make two different radial velocity measurements if they are not colocated. In this case, it is desirable to transmit both waveform types (SPY-1 and NEXRAD) from a single radar without any delay between the two and compare the results. In this experiment, software patches to the computer program which controls the radar allows SPY-1 to transmit an uncoded waveform which is very similar to NEXRAD's. In each beam position, SPY-1 is configured to transmit the NEXRAD waveform followed immediately (within milliseconds) by a SPY-1 waveform. The results from the two waveforms can then be compared for the entire search region.

Spectrum width measurements can be evaluated by using both ray trace comparisons with data tak-

en from SPY-1 alone, and from spectrum width maps taken from SPY-1 and NEXRAD.

## Results from two Precipitation Events:

Two sets of results are presented in this paper. One is from a precipitation event that passed through southern New Jersey on June 19, 1996. The other is from one which passed through on August 21, 1996. The June data is presented first. These data are typical of those collected throughout the summer collection events.

Two basic comparisons are presented in the June 19 data. First, a comparison is made between the spectral moment estimates made from an MTI waveform transmitted from the SPY-1 radar at CSEDS and the spectral moment estimates made from an uncoded NEXRAD dwell sequence from the same radar.

Figure 2 shows a comparison of reflectivity measurements from the MTI and NEXRAD waveforms. The estimates from the MTI waveform (solid line)

match well with the reflectivity estimates made a few milliseconds later with the NEXRAD waveform (dashed line). The estimates were averaged to a 1 kilometer range interval, typical of the reporting intervals required for most of the reflectivity based weather products used by the National Weather Service. It should be noted that the reflectivity traces match well even over steep gradients, such as the one located at the range interval between 10 and 13 kilometers. This is a reflectivity shift of approximately 35 dBZ. It is in steep gradient regions where range sidelobe corruption is expected to have the greatest impact on spectral moment measurements. The traces continue to match well over a low reflectivity region at a range of 39 kilometers, and over a variety of peaks and valleys. The variations between the SPY-1 waveform and NEXRAD waveform reflectivity estimates are reflective of the random nature of the weather phenomenon, and match the level of variance expected of these estimates.

Figure 2:

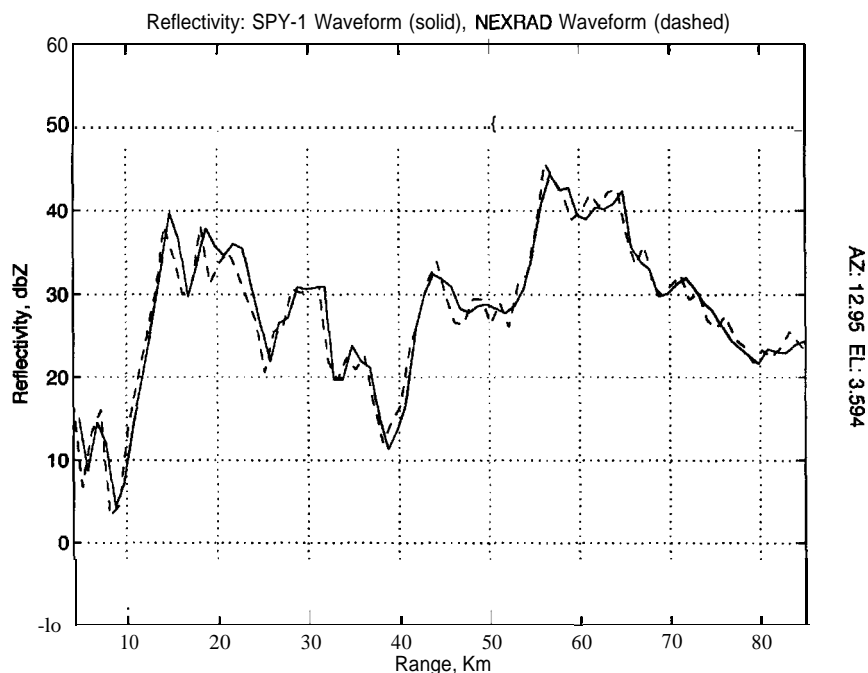
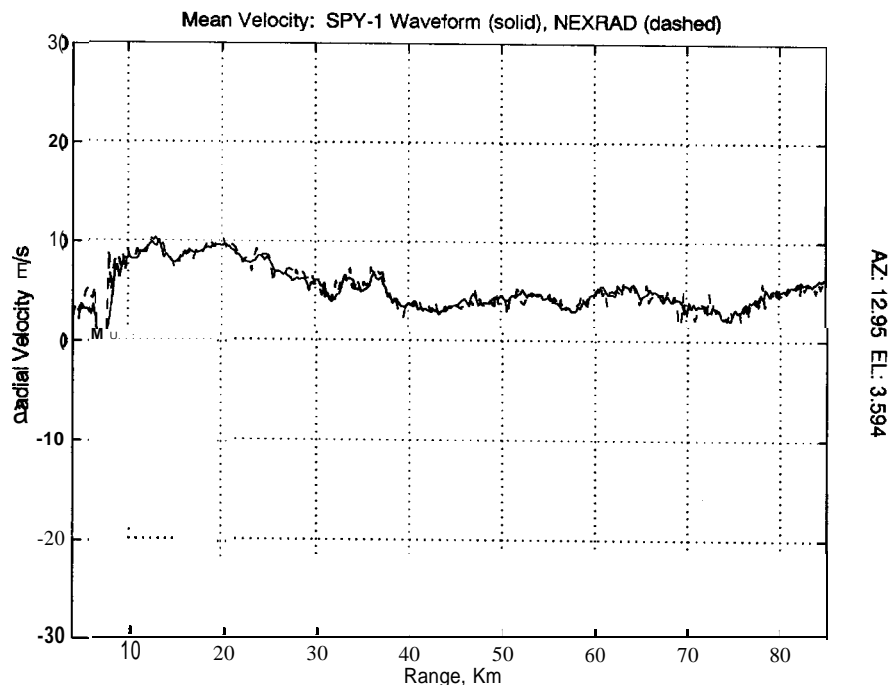


Figure 3 illustrates the performance of the mean velocity estimator for both the MTI waveform and a NEXRAD waveform transmitted from SPY-1. These radial velocity estimates were taken from the same pulses as the previously presented reflectivity estimates. Once again, the measurements made from the SPY-1 waveform match well with those from the NEXRAD uncoded waveform.

A number of detailed features can be seen along both radial velocity traces. The radial velocity values presented here are in meters per second (double these values to approximate speed in knots).

Figure 4 shows a comparison between spectrum width values generated by an MTI waveform and those generated from an uncoded NEXRAD waveform also transmitted from the CSEDS SPY-1 ra-

Figure 3:



alar. The MTI waveform values are represented by a solid line, and the NEXRAD waveform values are represented by a dashed line. The spectrum width estimation usually appears to have a relatively high variance (appears to be more noisy) than the other moments. However, both waveform types are reporting very similar values and the same trends over the full range interval. Large spectrum width values (indicating phenomena such as shear and turbulence) appear at approximately 8 kilometers. Small spectrum width values are reported by both waveforms at a range of approximately 55 kilometers.

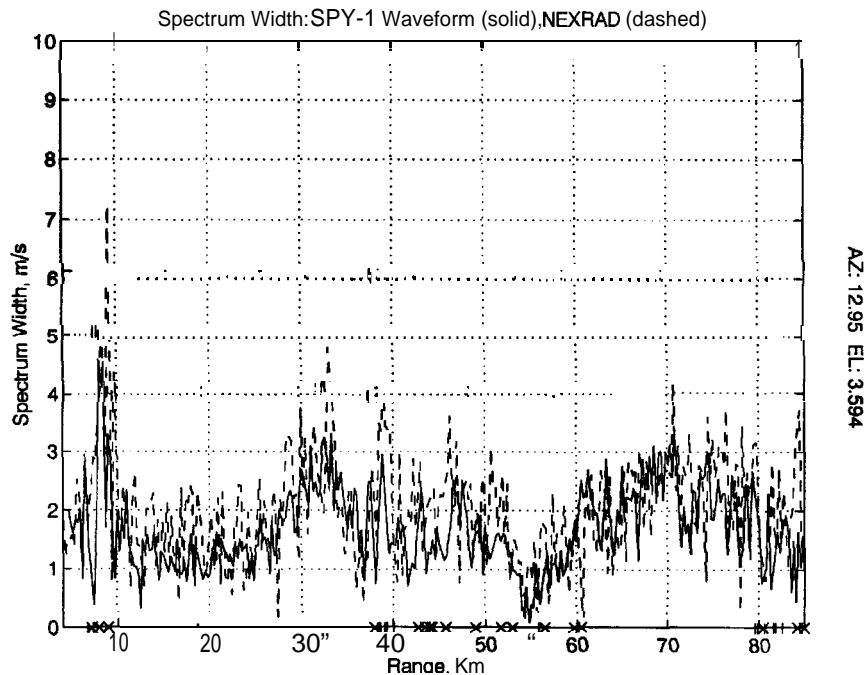
In the spectrum width calculation described previously, it is necessary to take the ratio of total signal power (total received power minus the receiver noise power) to the magnitude of the first lag of the autocorrelation function. Since the estimated receiver noise is subtracted from total noise power, and since the total received power is an estimate with a nonzero variance, sometimes the result is that the total signal power value is actually smaller than the absolute value of the first lag. In theory this is impossible, but it occurs as a result of the errors inherent in any measurement where noise is present. Therefore, sometimes the spectrum width value may not be a valid one. In these cases, the value is flagged and not used.

In the spectrum width comparison shown here, these invalid estimates are marked with an "x" for the NEXRAD waveform and with a small vertical

line for the SPY-1 waveform, along the x-axis of the plot. Over a 10 kilometer region forty estimates are displayed. On average approximately three or four estimates (for the NEXRAD waveform -- one or two for the SPY-1 waveform) are invalid and thrown away. This means that over 90% of the estimates are valid in this plot.

The next results presented involve entire maps of spectral moment estimates. They are displayed using the National Weather Service's WVS display package. In the first two color figures included at the end of this paper (Figures 5 and 6), maps of radial velocity are displayed for the same scan from which the previously discussed ray traces were taken. The first figure is a map of SPY-1 waveform radial velocity estimates taken at an elevation of 3.6 degrees. The range rings are provided 30 kilometers apart (measurements are shown out to approximately 90 kilometers). On the second plot the radial velocity estimates from the NEXRAD waveform are displayed. The green regions indicate a radial velocity inbound to the radar at approximately two meters per second. The white region indicates zero radial velocity (all motion is tangential to the radar). The dark brown region indicates an outflow of approximately four meters per second. The lighter brown region shows outflows of seven meters per second, and occasional orange pixels indicate an outflow of eleven meters per second.

Figure 4:



The two plots are nearly identical. Small regions of inflow occur directly north of the radar, with tangential flow just to the right of these regions. The wind fields show an outflow which increases as the radar scans to the East. Detailed features visible in the white regions, and between the brown shaded regions, are clearly visible in both plots. Overall, the wind field illustrated by the SPY-1 MTI waveform matches very well with that of the NEXRAD uncoded pulse doppler waveform. The MTI waveform reduces the data collection time for the volume by more than an order of magnitude. Both radial velocity plots generally agree with storm motion indicated by storm cell movement and by radial velocity plots provided by the nearby NEXRAD.

The last three color pictures, figures 7-9, illustrate a series of reflectivity maps from an August storm. Since the SPY-1 radar has an agile beam with a flexible scan, and since the MTI waveform can make radial velocity measurements with an order of magnitude reduction in time, the SPY-1 radar is capable of generating accurate, rapid snapshots of storm events not possible by rotating parabolic antenna radars such as NEXRAD.

Figure 7 is a composite reflectivity plot generated from SPY-1 MTI data. In composite reflectivity maps, the largest reflectivity value from any altitude at a given geographic position is reported as the composite reflectivity for that position. The reports are made on a Cartesian grid with a 1 kilometer grid spacing. The brown region indicates high

reflectivity values of approximately 43 dBZ. The white regions show reflectivity values of 38 dBZ. The green regions vary from 33 to 23 dBZ. And the blue regions go down to 8 dBZ (light rain). Below this point, the SPY-1 reflectivity maps are thresholded (although these values are still well above the receiver noise floor). This is done to keep the results unclassified and still provide valid, useful measurement data.

This data was collected over a time interval less than 10 seconds. The extent of the reflectivity map is limited only by the experimental data collection device used in the mission (in real operation, such a radar would be able to provide 360 degrees of coverage). The range rings are provided 30 kilometers apart, with the first ring visible corresponding to a range of 60 kilometers, relative to SPY-1. The azimuth mark in the figures correspond to 30 degrees from North.

Two distinct cells are visible in the first figure. They are relatively small (1 to five pixels in size for the brown region). Velocity plots from the day indicate general storm motion was going from West to East.

The second SPY-1 plot (figure 8), was taken 2.5 minutes later. The same two cells, as well as other distinct matching features, appear. They are still small in size, and the centroids have moved just under 2 kilometers eastward (indicating a speed of approximately 12 m/s, or about 24 knots).

The last color plot, figure 9, shows the composite reflectivity map taken from the nearby NEXRAD

radar located approximately 43 kilometers to the SSW of the two dominant cells near the center of the screen. The NEXRAD radar is closer to the storm cells than the SPY-1 radar is. The map is generated with the same composite reflectivity calculation, and with the same grid spacing. The azimuth and range rings in this plot are centered on the SPY-1 radar located at the CSED Site. The scan used to collect the NEXRAD data took approximately 5 minutes, a significantly slower scan than that of the SPY-1 radar. The region scanned by SPY-1 is shown with a dark border. The two cells in this plot clearly correlate to the two cells in figures 7 and 8. The other general features of the green and blue regions also correlate well to figures 7 and 8. However, the main cell is significantly larger in size and almost appears as one cell. This cell appears smeared because of the effect that the slower NEXRAD scan has on the composite reflectivity calculation used to generate the images in Figures 7-9. Combination of Figures 7 and 8 results in a cell which more closely resembles that of Figure 9. The temporal resolution gained with an agile beam radar using range averaging also improves the spatial resolution which results from calculations such as composite reflectivity.

## Conclusions:

Detailed analysis of the data continues. Efforts are focused on identifying and analyzing especially stressing cases, such as when measurements are being made near fast point targets or when steep reflectivity gradients occur. With a preliminary analysis complete, however, several main conclusions can be drawn from this work.

MTI waveforms, using small numbers of pulses (such as 3 and 4 pulse MTI systems), can provide accurate measurements of the three spectral moments typically observed by radar meteorologists. The results from this experiment show that measurements taken from a SPY-1 radar compare favorably with those taken from a NEXRAD or those taken using the NEXRAD uncoded pulse sequence transmitted by a SPY-1. This means that tactical radar systems can provide valuable weather data without interrupting their normal tactical search scans.

Another advantage of this processing approach is that the shorter dwells, typical of tactical systems, can provide these measurements very quickly. When this is combined with the fact that many tactical systems use flexible electronic scan tech-

niques, very rapid updates can be provided of developing weather conditions.

Dedicated weather dwells will be required for certain types of information. When surface clutter interferes with weather signal returns, a longer dwell sequence is required to filter the surface clutter from the weather signal. Also, when clear air observations are desired, longer pulse sequences are required to allow the typical tactical system to achieve the required sensitivity. Implementation of infrequent dedicated dwells, however, have less of an impact on agile beam tactical systems such as SPY-1. In such systems, they can be transmitted, on a low priority basis, when the tactical system can afford to schedule them. In tactically critical situations where no radar resources are available for any dedicated weather scan, they can be eliminated entirely.

Future work on this experiment will include investigations into making clear air observations with the SPY-1 radar.

## Acknowledgements:

The authors thank Dr. Scott Sandgathe of ONR for sponsoring this work. Also, we would like to thank the AEGIS Program Office for providing the SPY-1 resources which made this experiment possible, and to the CSED Site personnel who assisted in the data collection events. We are grateful to Dr. Frank Herr from ONR and CDR Markham from NRL for their support of the program, and to Dr. Juergen Richter of NRaD for his contributions as technical advisor to the experiment. And we would like to thank the personnel from the National Weather Service's Mount Holly, NJ office for their outstanding support, and the National Center for Atmospheric Research for their support and use of their RDSS display software package.

## References:

- [1] R. Doviak and D. Zrnic, *Doppler Radar and Weather Observations*, New York: Academic Press, Inc., 1993.
- [2] R. J. Keeler and C. L. Frush, "Rapid Scan Doppler Radar Development Considerations, Part II: Technology Assessment", *Proceedings 21st Conference on Radar Meteorology*, AMS, Edmonton, Canada, 1983, pp 3.1-3.5.
- [3] H. Urkowitz and N. Bucci, "Doppler Tolerant Range Sidelobe Suppression in Pulse Compression Meteorological Radar", *Proceedings International Geoscience and Remote Sensing Symposium 92*, Houston, TX, May 26-29, 1992, Vol. I, pp. 206-208.



[4] R. Nevin, J. Ashe, N. Bucci, H. Urkowitz, and J. Nespor, "Range Sidelobe Suppression of Expanded/Compressed Pulses with Droop", *Proceedings 1994 /IEEE National Radar Conference, Atlanta, GA, March 29-31, 1994*, pp. 116-122.

[5] N. Bucci, J. Nespor, H. Urkowitz, D. Mokry, R. Brown, W. Baldygo, "An Experiment with an S-Band Radar Using Pulse Compression and Range Sidelobe Suppression for Meteorological Measurements", *Proceedings 1994 IEEE National Radar Conference, Atlanta, GA, March 29-31, 1994*, pp. 35-40.

[6] N. Bucci, J. Nespor, and H. Urkowitz, "Use of Pulse Compression and Range Sidelobe Suppression for Meteorological Radar Measurements at S- and X-Band", *Proceedings International Conference on Advanced Radar Meteorology, COST 75, Brussels, Belgium, September, 1994*.

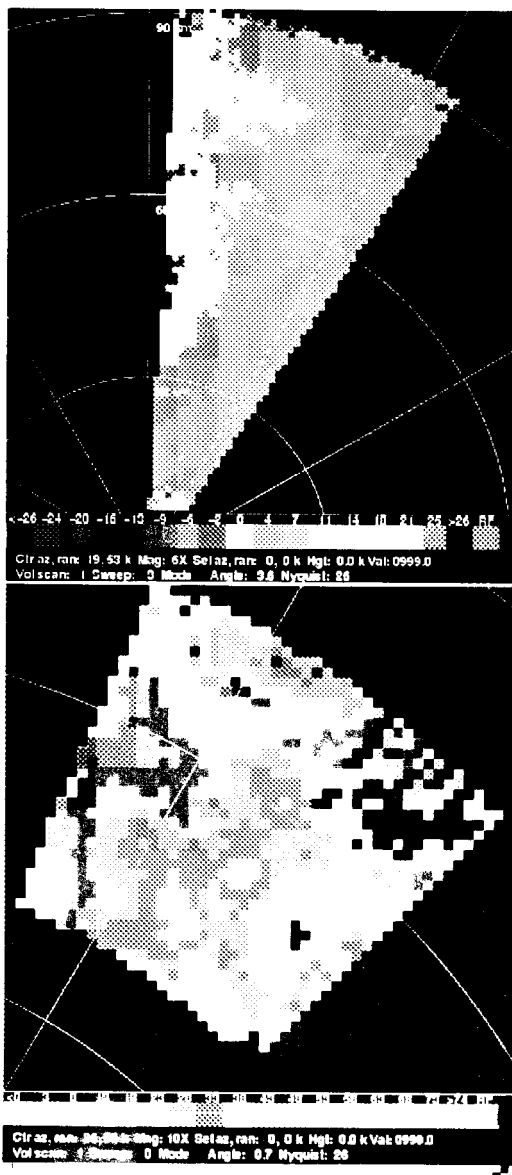


Fig 5

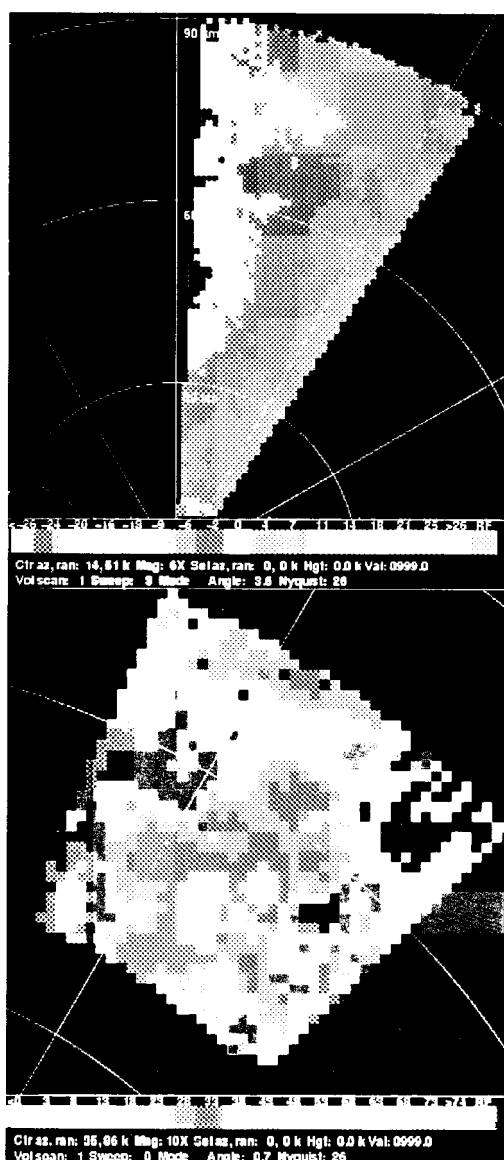


Fig 6



Fig 7

Fig 8

Figure 5: Radial Velocity Map, 3.6 deg. el., taken from SPY-1 using MTI Waveform

Figure 6: Radial Velocity Map, 3.6 deg. cl., from SPY-1 using NEXRAD Waveform

Figure 7: Rapid Composite Reflectivity Snapshot Taken by SPY-1 Using MTI Waveform

Figure 8: Second Rapid Composite Reflectivity Snapshot Taken by SPY-1 Using MTI Waveform

Figure 9: Composite Reflectivity Picture From NEXRAD, Located Approx. 44 Km to East of SPY-1